X-ray reflectivity study of a W/Si multilayer grating

M. Jergel[1], C. Falcony
Departamento de Física, CINVESTAV-IPN, Apdo Postal 14-740, 07300 México, D.F., México

P. Mikulík[2]
Fraunhofer Institut für Zerstörungsfreie Prüfverfahren, EADQ, Krügerstr. 22, D-01326 Dresden, Germany

L. Ortega
Laboratoire de Cristallographie du CNRS, BP 166, 38042 Grenoble, France

E. Majková, E. Pinèík, Š. Luby
Institute of Physics, Slovak Academy of Sciences, Dúbravská cesta 9, 842 28 Bratislava, Slovakia

I. Kostiè, P. Hudek
Institute of Informatics, Slovak Academy of Sciences, Dúbravská cesta 9, 842 37 Bratislava, Slovakia

Multilayer gratings are artificially patterned multilyer thin films with the periodicities both in the lateral and normal directions which renders them attracting for microelectronic and optical applications. A proper structural characterization is of primary importance. To test the capability of the X-ray reflectometry technique to fulfil this task, a tungsten/silicon multilayer grating prepared by electron beam evaporation and electron beam lithography was studied both in the coplanar and non-coplanar geometries., the nominal lateral and normal periods being 800 nm and 8 nm, respectively. The coplanar measurements were evaluated within the dynamical theory of X-ray scattering on rough gratings and provided the structural parameters of a real structure with a reasonable precision which are close to the nominal ones. The results revealed also some imperfections of the deposition and masking procedures which are discussed. The non-coplanar measurements were evaluated qualitatively using three-dimensional constructions in the reciprocal space. The advantage of the technique used is its non-destructive character and a simultaneous access both to the surface shape of the grating as well as to its internal structure.

Keywords: Multilayer grating; Quantum wires; Lateral diffraction; Grating truncation rods; X-ray reflectivity; GISAX

1. Introduction

Multilayer gratings (MLGs) are thin film structures with the periodicities in both the lateral and normal directions. The lateral periodicity comes from a regular alternating of the grooves and wires along the surface while the normal one stems from a periodic stacking of the layers of two different compositions inside the wires (Fig. 1). MLGs hold great potential for the applications in micro- and optoelectronic devices (e.g. quantum wires, coupling elements in surface lasers) and optical elements for soft X-ray and ultraviolet region (e.g. monochromators, dispersion elements with a constant resolution) where no natural lenses and mirrors are available. In electronic applications, one-dimensional electron confinement is responsible for unique MLG properties while in optics, high throughput and high spectral resolution are combined together due to two periodicities present. The perfection of the MLG structure is crucial for achieving the desired properties. Therefore, a proper structural characterization is inevitable to provide a necessary feedback for technology. The aim of this paper is to study the grazing-incidence small-angle X-ray scattering (GISAX) effects specific to MLGs in different measurement geometries in order to utilize them for a detailed analysis of the real structure. Hard X-rays of the wavelength between 0.1 – 0.2 nm were used.

2. Experimental

MLG structures may be obtained by lateral patterning of planar multilayers on a mesoscopic (sub-micrometer) scale. Therefore, the sample was prepared in three steps. First, a planar multilayer was deposited by electron beam evaporation in ultra high vacuum of 10^{-7} Pa (UMS 500 Balzers) of alternating W (nominal thickness 7 nm) and Si (1 nm) layers onto Si(100) wafer covered with a 0.3 μm thick SiO_2 oxide, the number of W/Si bilayers being 10. In the second step, a grating mask was produced on the multilayer surface by electron beam lithography. A three-level mask consisting of polyimide (PI) on the multilayer, amorphous Si in the middle and poly-methyl-methacrylate (PMMA) on the top was used. The MLG mask with 800 nm lateral period was first prepared from the top PMMA layer by rectangular shots of 5 μm × 300 nm (ZBA 10/1 direct-write vector-scan pattern generator Carl Zeiss). Subsequently, it was transferred into the amorphous Si layer beneath by the reactive ion beam etching in CF_4 plasma and afterwards into the PI layer by an oxygen

[1] on the leave from the Institute of Physics, Slovak Academy of Sciences, Bratislava, Slovakia
[2] on the leave from the Laboratory of Thin Films and Nanostructures, Masaryk University, Brno, Czech Republic

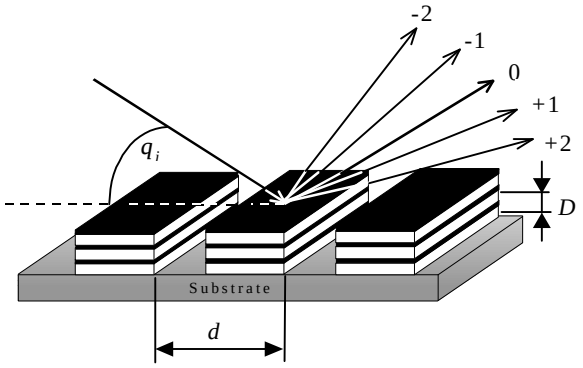

Figure 1. A schematic view of a multilayer grating. *d* and *D* are the lateral and normal periods, respectively. An X-ray beam incoming under the angle of incidence q_i is simultaneously diffracted into a fan of grating diffractions of different orders around the specular beam.

plasma process. In the last step, Ar^+ ion beam etching (LPA USI Model Ionic) through the mask prepared and across the whole multilayer provided the final MLG structure. The residual resist was removed by standard dry and wet procedures.

The X-ray measurements in the plane of incidence (coplanar geometry) were performed on a four-circle diffractometer. The radiation was delivered by a Rigaku 12 kW rotating anode generator and monochromatized at the 0.15418 nm wavelength (CuK_α) by a graphite monochromator, the primary beam having been restricted by a 30 μm slit. A NaI(Tl) scintillation counter with an 80 μm slit was used for the detection. The use of an intense X-ray source is even more important for the measurements out of the plane of incidence (non-coplanar) where the scattering effects are rather weak. These measurements were performed at the European Synchrotron Radiation Facility (Grenoble, France), beamline ID1, at the wavelength of 0.161 nm. A two-dimensional gas-filled detector with the resolution of 1024^2 pixels and the dimension of 20×20 cm^2 was positioned perpendicularly to the plane of incidence at a variable distance from the sample ranging from 80 cm to 450 cm. The whole experimental set-up was in a vacuum vessel to avoid the air scattering. To protect the detector against the intense specular reflection, an absorbing needle was placed in front of its central part.

3. Reciprocal space considerations

Reciprocal space enables us to study scattering effects in a rather transparent geometrical way. A real structure is represented here by a corresponding reciprocal lattice. The constructive interference (diffraction) occurs when a point of the reciprocal lattice gets on the Ewald sphere of the radius $2\pi/l$ with its centre being controlled by the incoming wave vector direction (l being the wavelength). The outgoing wave vector (diffraction direction) connects the centre of the Ewald sphere and the point on its surface.

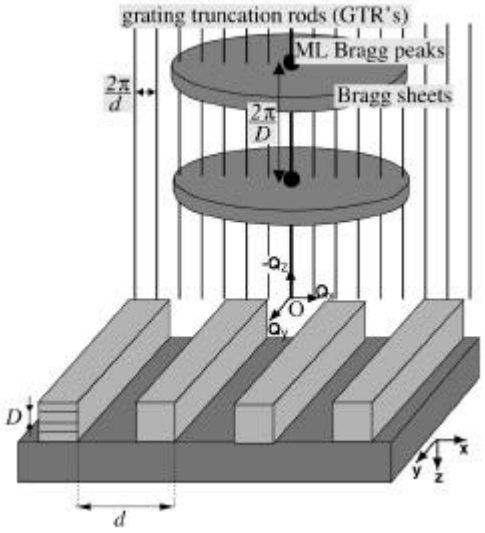

Figure 2. Real and reciprocal space representations of a multilayer grating with rough interfaces

Thus the reciprocal lattice is directly related to the spatial distribution of the scattered intensity.

The reciprocal lattice of a MLG and its relation to the real structure is shown in Fig. 2. The lateral periodicity is manifested in the reciprocal space by a set of equidistant grating truncation rods (GTRs) displaced by $2\pi/d$, *d* being the lateral period. The GTRs are located in the plane which is perpendicular to the mean MLG surface and to the wires at the same time. The normal periodicity inside the wires produces modulations of the scattered intensity profile along the GTRs with the multilayer Bragg maxima displaced equidistantly by $2\pi/D$, *D* being the normal period. Moreover, sheets of an enhanced intensity appear spreading across Bragg maxima of different orders. This effect, called resonant diffuse scattering (RDS), stems from the constructive interference of the X-rays scattered diffusely on rough multilayer interfaces with at least partly replicated morphology inside the wires [1].

There are two limiting cases to study scattering effects, namely when the plane of incidence of the X-rays is parallel (azimuth $j = 0°$) or perpendicular ($j = 90°$) to the wires. Between them, the effective grating period $d/\sin j$ in the plane of incidence changes from infinity to *d*. A scheme of the latter case, mostly used in optical applications, is shown in Fig. 3. Here, the GTRs plane coincides with the plane of incidence. Therefore, a certain number of the MLG diffractions around the specular beam, depending on the angle of incidence q_i, are excited simultaneously into the directions where the Ewald sphere crosses particular GTRs. These MLG diffractions are coplanar. Out of the plane of incidence, non-coplanar part of the RDS sheets occurs. The situation with the plane of incidence directed along the wires is shown in Fig. 4. Here, the plane of incidence is perpendicular to the GTRs plane so that the Ewald sphere crosses the GTRs non-coplanarly except that of the zero order (specular GTR). Consequently, a fan of the MLG diffractions is excited simultaneously out of the

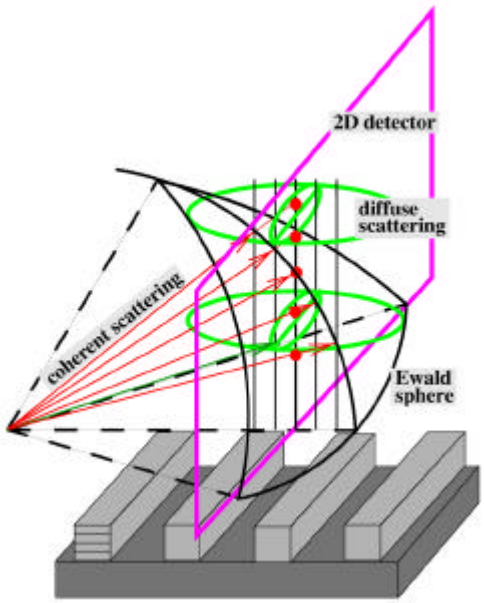

Figure 3. Reciprocal space construction for the plane of incidence perpendicular to the wires (azimuth j = 90°).

plane of incidence, their number being $(2d/l)\sin q_i$. These diffractions are accessible in the non-coplanar measurement geometry. Again, the RDS sheets are present out of the plane of incidence. They are insensitive to the sample azimuth provided the interface roughness is isotropic.

The behaviour of the GTR diffractions in both geometries discussed above follows directly from the continuity of the incident and scattered X-ray wave fields across the MLG surface.

4. Coplanar measurements

The coplanar measurements were performed with the plane of incidence perpendicular to the wires (j = 90°). First, the cut of the reciprocal space in this plane (coplanar reciprocal space map) was measured directly as a set of the sample rocking curves (trajectory in the reciprocal space parallel to the Q_x axis,. Fig. 5). The GTRs are visible up to the 5th order as well as the cross-sections of the RDS sheets. These sheets are not planar but bent due to the refraction and follow the contours of the limiting Ewald spheres. Inside them, there is no scattered intensity. An example of the rocking curve measured across the 2nd order Bragg maximum is shown in Fig. 6. In addition to the regular GTRs, parasitic GTRs are visible in between. They are due to some repeating irregularities of the wire width (lateral superperiodicity) during the mask production. An analogous rocking curve measured on the planar multilayer (before the etching) is shown for comparison.

From the GTRs distance, the lateral period d = 798 nm follows which is very close to the nominal value of 800 nm. Further MLG structure parameters may be extracted from fitting the intensity modulations along the GTRs by a matrix modal eigenvalue approach of the dynamical theory of X-ray scattering on rough gratings [2,3] as it has been

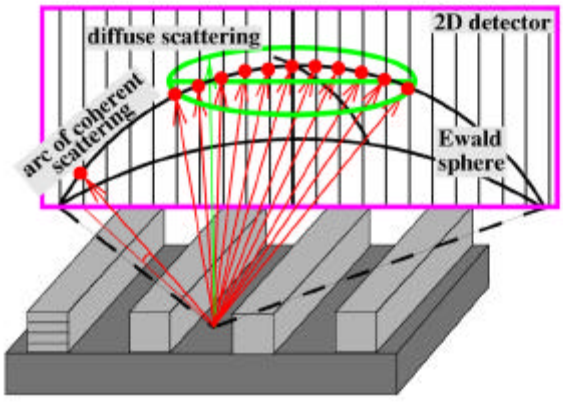

Figure 4. Reciprocal space construction for the plane of incidence parallel to the wires (azimuth j = 0°).

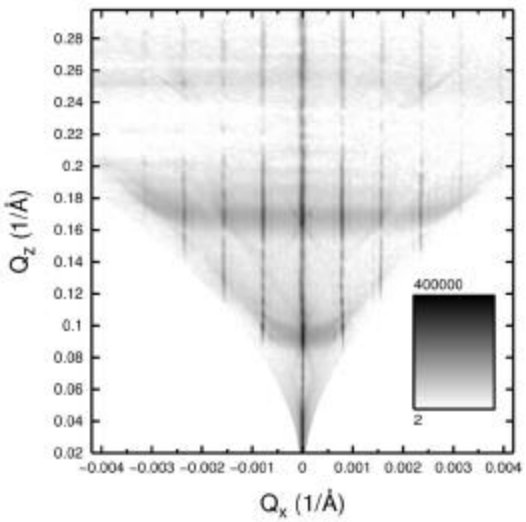

Figure 5. Reciprocal space map of the grating measured in the coplanar geometry with the azimuth $j = 90°$. Q_x and Q_z are the lateral and normal components of the wave vector transfer, respectively.

shown previously [4]. These modulations are visible in Fig. 5 and were measured also separately, Fig. 7. While the wire width to grating period ratio affects the envelope of the intensities of the GTRs of different orders along Q_x axis at a constant Q_z, the layer thickness ratio inside the wires controls the intensity modulations along the GTRs. Both ratios together determine the average density of the MLG which controls the position of the critical angle for the total external reflection on the zero order (specular) GTR and the first sharp peak position on the non-zero GTRs. The large GTRs modulations are Bragg maxima and smaller ones are due to the limited wire thickness (Kiessig fringes). Bragg maxima are asymmetric and broaden with the increasing order which indicates a variable normal period D upwards the wires. The fit revealed the values of 7.1 nm and 7.6 nm at the substrate and surface, respectively. This fact is obviously due to a slight instability of the deposition parameters. The W layer thickness inside the wires was found to be (1.1 ± 0.2) nm but the thickness of the uppermost W layer on the wire surface was reduced. In fact, this layer was oxidized in the planar multilayer and probably reduced during the resist removal in the MLG. It is known that tungsten oxides have a low mechanical compatibility and some of them are volatile at elevated temperatures. Further, the interface roughness of (0.5 ± 0.2) nm and wire width to period ratio of 0.61 ± 0.02 were determined from the fit.

5. Non-coplanar measurements

The main advantage of the non-coplanar geometry lies in the possibility to span much larger interval of the lateral component of the wave vector transfer Q_x as the limitations imposed by the Ewald sphere, inherent to the coplanar geometry, are absent here. The non-coplanar measurements

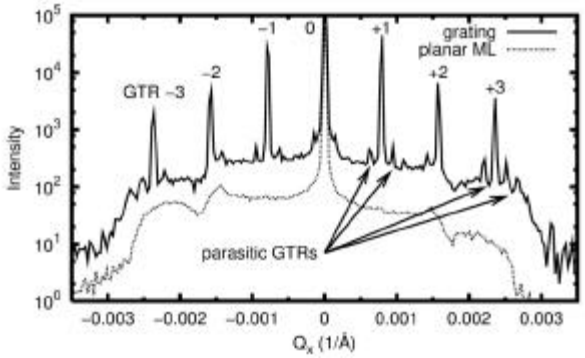

Figure 6. Rocking curves neasured across the 2nd Bragg maximum of the multilayer grating and planar multilayer before the etching, the latter curve being shifted downwards for the sake of clarity. In addition to the regular grating truncation rods, parasitic ones can be seen in the former curve which are due to patterning imperfections.

were first performed with the plane of incidence perpendicular to the wires ($j = 90°$, Fig. 3) at different angles of incidence. An example is shown in Fig. 8. This image represents the projection of the intersection of the reciprocal lattice of the MLG with the Ewald sphere onto the detector plane. Note that there is a shadowing effect from the sample as the sample horizon moves upwards with the increasing angle of incidence. In the central part, the shadow of the absorbing needle is visible. It coincides with the projection of the plane of incidence, identical with the GTRs plane, onto the detector plane. Therefore, the coplanar MLG diffractions are not visible here. The non-coplanar scattering is purely diffuse so that the RDS sheet projections can only be seen out of the plane of incidence.

An image taken with the plane of incidence along the wires ($j = 0°$, Fig. 4) is shown in Fig. 9. The Ewald sphere

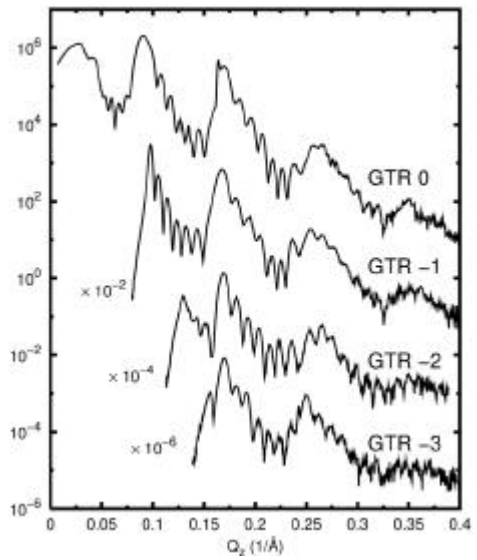

Figure 7. Measured grating truncation rods of different orders. The zero order (specular) truncation rod is a counterpart of the specular reflectivity of the planar multilayer.

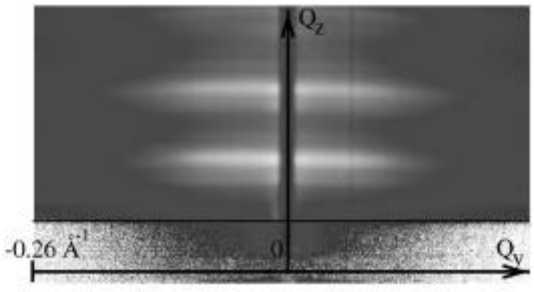

Figure 8. Image of the scattered intensity recorded by a two-dimensional detector located 150 cm from the sample with the angle of incidence $q_i = 0.351°$ and the azimuth $j = 90°$.

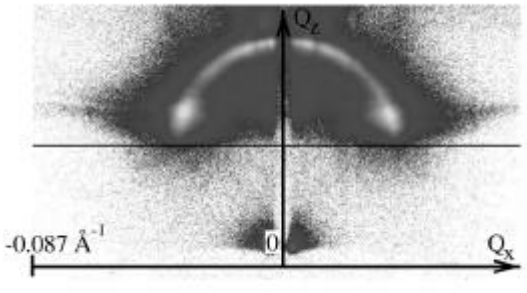

Figure 9. Image of the scattered intensity recorded by a two-dimensional detector located 450 cm from the sample with the angle of incidence $q_i = 0.47°$ and the azimuth $j = 0°$.

crosses here the GTRs out of the plane of incidence and the simultaneously excited GTR diffractions intersect the detector plane in the form of an arc above the sample horizon. We found that its shape is very sensitive to the azimuth j which was set with the precision of 0.01°. The angular resolution of the detector depends on the pixel size and the distance from the sample. It was not sufficient to distinguish particular GTR diffractions even with the largest distance used so that the arc is more or less continuous. In the case shown, there are 80 GTRs excited simultaneously. They all are very intense which indicates a strong inter-truncation scattering. Bright spots at the extremities of the arc are visible corresponding to the MLG diffractions exiting close to the critical angle. This phenomenon is analogous to the Yoneda effect observed on the rough planar surfaces (surface resonant scattering).

6. Conclusions

The GISAX effects specific to the MLG structure were measured in the coplanar and non-coplanar geometries. An intense X-ray source is inevitable for such measurements to provide meaningful data for the analysis. The coplanar measurements were evaluated quantitatively within the dynamical theory of X-ray reflection from rough gratings to extract the parameters of the multilayer stack inside the wires and the wire width to period ratio. The coplanar measurements revealed also some imperfections of the multilayer deposition and the patterning procedure giving a useful feedback for the technology. The non-coplanar measurements were performed with different MLG azimuths. The results were analyzed qualitatively by the constructions in the reciprocal space and confirmed the theoretical expectations. A quantitative evaluation of the non-coplanar MLG diffractions is the task for the future. Our results suggest strong inter-truncation rod scattering, hence, the use of the dynamical theory will be necessary also here.

Acknowledgements

The authors acknowledge a partial support from the Scientific Grant Agency VEGA, Bratislava, grant no. 2/7103/20. P.M. acknowledges support by a Marie Curie Fellowship of the European Community programme “Human Potential” under contract no. MCFI-2000-00671.

References

[1] V. Holý, T. Baumbach, Phys. Rev **B 49**, 10668 (1994).
[2] P. Mikulík, T. Baumbach, Phys. Rev. **B 59**, 7632 (1999).
[3] T. Baumbach, P. Mikulík, in *X-ray and Neutron Reflectivity Principles: Principles and Applications*, ed. J. Daillant and A. Gibaud, Springer Verlag, Berlin 1999, p. 232.
[4] M. Jergel, P. Mikulík, E. Majková, Š. Luby, R. Senderák, E. Pinèík, M. Brunel, P. Hudek, I. Kostiè, and A. Koneèníková, J. Phys**. D 32**, A220 (1999).